EPiC Series in Technology
Volume 4, 2026, Pages 65–74
Proceedings of The 11th International Conference on Tribology in Manufacturing Processes & Advanced Surface Engineering

Tribological Control in Adaptive Die Systems for Cold Forging: Investigation of Tribological Influence on Ejection Force Reduction

Christian Siedbürger[1], Christoph Kuhn[1] and Peter Groche[1]
[1] Institute for Production Engineering and Forming Machines (PtU), Otto-Berndt-Straße 2, 64287 Darmstadt, Germany
christian.siedbuerger@ptu.tu-darmstadt.de, christoph.kuhn@ptu.tu-darmstadt.de, groche@ptu.tu-darmstadt.de

Abstract

In cold forging, ejection forces are a key indicator of the tribological state and tool wear, as they are largely governed by the clamping pressure resulting from elastic die springback after the main forming stroke. This study investigates how an adaptive extrusion die reduces the external pressure, thereby lowering the clamping pressure and positively affecting ejection forces. A two-step model has been developed in a tribometer to represent the ejection stage. This test reproduces the tribological preloading from the main forming operation, as well as the reversal of motion under varying contact pressure. The findings from this test are transferred to the real process by finite element simulations. The results reveal a pressure-depending friction trend for polymer-based single layer lubricants in the reverse stroke, such that reducing contact pressure is accompanied by a decrease in the friction coefficient. Consequently, the beneficial effect of the adaptive die on ejection forces is not only caused by reduced clamping pressure but is further amplified by a reduction in friction. This indicates that adaptive tooling systems can contribute effectively to increased tool life.

1 Introduction

Cold forging is a subgroup of bulk metal forming that enables the high-volume production of axisymmetric components with high dimensional accuracy and surface quality. The process is characterized by severe tribological loading on both the tool and the billet, with normal contact pressures reaching up to 3,000 MPa and surface enlargements of up to approximately 3,000 % [1]. Under these conditions, lubricant systems play a key role because they must maintain separation of the contact partners and thereby mitigate premature tool damage caused by adhesive and abrasive wear. A practical process metric for assessing the tribological state and the associated tool wear is the ejection force, as encountered in forward extrusion or tapering operations [2]. After forming, the part has to be released from the die against the clamping pressure that builds up in the forming cavity. When the punch load is removed, the die recovers elastically in the radial direction due to the previously introduced elastic strains, which increases the clamping of the part. Consequently, the ejection force is largely governed by sliding and adhesive friction during ejection [3]. In industrial process chains, the measured ejection force can be used as an indicator of the tribological condition, since elevated ejection forces typically correlate with higher friction coefficients and progressive degradation of the tool contact [4]. For example, studies have shown that the effective friction coefficient at the internal tool surface can double after 100,000 strokes in continuous operation, due to progressive wear and the associated roughening of the tool–workpiece contact surfaces [4]. Because the ejection stage imposes an additional load on the applied lubricant system beyond that of the main forming operation, this effect accumulates particularly in multistage cold forming process chains. It can markedly reduce the operating window of the tribological system, thereby adversely affecting process economics [1, 5]. Accordingly, process design and operation aim to minimize ejection forces by selecting appropriate lubricants, tool coatings, and wear oriented tooling concepts to increase tool life and process stability.

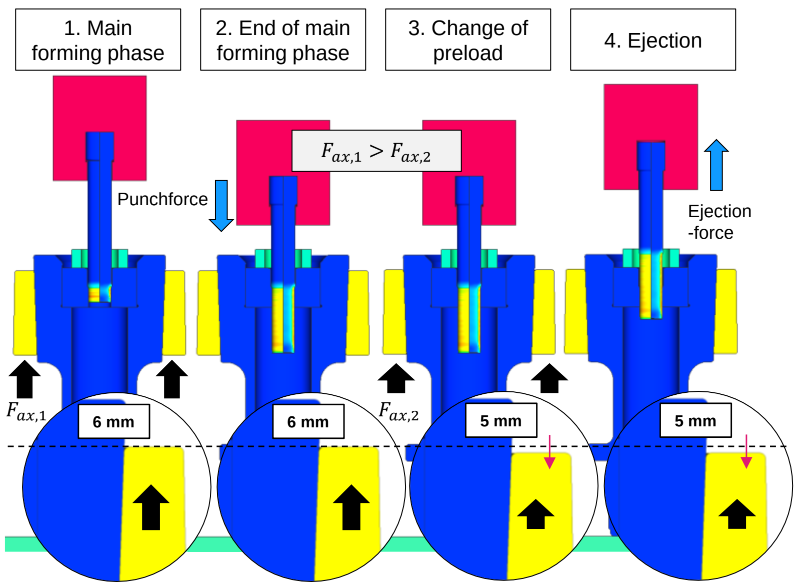

Figure 1 Adaptive die tooling concept. Left: Assembly of the adaptive die system with all relevant components. Right: Process sequence illustrating the preload adjustment within process phases 1 – 4 by the active reinforcement.

One promising approach to reducing ejection forces and thereby improving tool life is the use of an adaptive extrusion die, as shown in Figure 1 [6]. Previous work has demonstrated that a targeted adjustment of the external pressure can reduce the elastic die recovery after forming. This lowers the clamping pressure acting on the part and consequently decreases the ejection forces [7]. The concept is realized by a conical wedge reinforcement system that, supported by an additional actuator, enables controlled radial die actuation [8]. The main ram performs the forward extrusion stroke to generate the taper, while the billet is clamped at the head so that ejection is realized by pulling the punch, see Figure 1. However, the scientific question remains open as to how the reduction in clamping pressure affects the tribological response of a lubricant system that has already been preloaded by the main forming stroke. The literature provides extensive investigations on the influence of surface topography, temperature, contact pressure, and surface enlargement and on their incorporation into friction models for finite element simulations of the main forming stage. The critical ejection stage, however, and in particular the reversal of sliding direction under preloaded contact conditions, is often neglected in these modeling approaches [1, 5, 9, 10]. Against this background, the present study develops a dedicated model test using a tribometer that reproduces both the tribological preloading from the main forming operation and the modified boundary conditions associated with reduced clamping pressures enabled by the adaptive tooling concept. The two-stage test sequence enables the systematic investigation of the tribological behavior during reversal of motion while independently varying the contact pressure level. Based on the experimental results, a correction approach for the friction coefficient specifically for the ejection stage is derived and verified by corresponding finite element simulations.

2 Material and Methods

The experimental program was conducted using case hardening steel 16MnCr5 (1.7131) and 42CrMo4 (1.7225) in semi-finished condition. To minimize batch related inhomogeneity and to obtain reproducible mechanical response, all billets were soft annealed in a furnace at 700 °C with a holding time of 8 h. After heat treatment, the specimens were sand blasted to increase the effective surface area and to promote lubricant adhesion. A final chemical cleaning step was applied to remove residues and to ensure consistent tribological boundary conditions prior to lubricant application. For surface conditioning, single-layer lubricant systems provided were investigated.

The original forming operation in the adaptive tooling system is a tapering process of an axisymmetric billet, where the diameter in the extrusion zone is reduced from 13 mm to 12 mm, see Figures 1 and 2. The clamping pressure is adjusted by actively modifying the die preload using conical reinforcement. The extrusion die is supported in a segmented sleeve that acts as the counter element to the active reinforcement. The segmented design reduces the resistance against axial actuation of the movable reinforcement. Mechanically, the system corresponds to a conical wedge transmission that converts axial actuation into radial die displacement and thereby sets the external pressure σ_N acting on the extrusion die. [7, 8, 6]

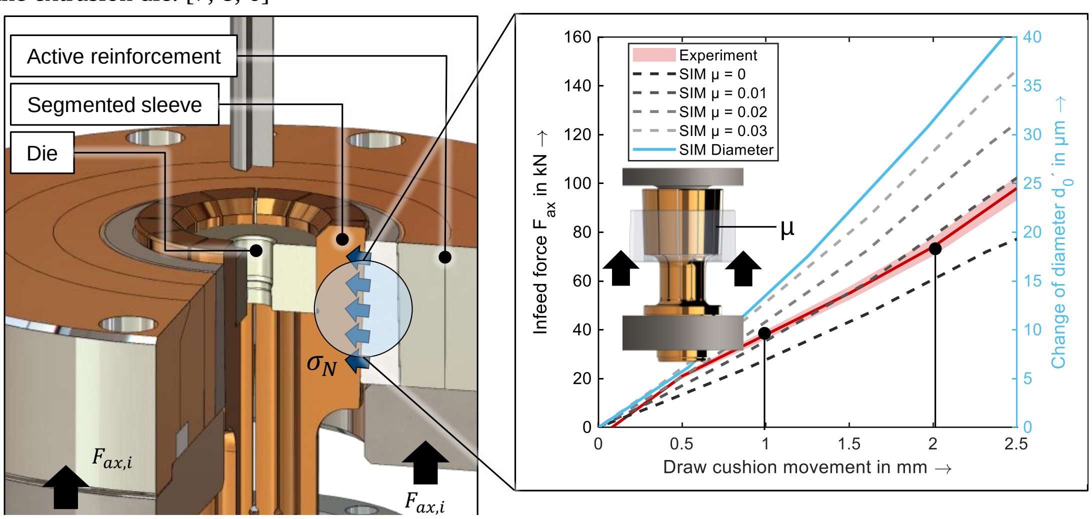

Figure 2 Infeed curve of the adaptive die used to adjust the external pressure acting on the die insert. The infeed characteristic is derived from preliminary experiments and validated against corresponding 2D FE simulations.

The tooling concept was implemented on a servo spindle press with a maximum press capacity of 2,500 kN. This configuration allows the press-integrated drawing cushion to serve as a second actuator for axial infeed of the movable reinforcement. To ensure comparability, the forming process was reproduced in a two-dimensional FE simulation based on a preceding publication. Simulations were performed in Simufact Forming using the implicit solver with quadrilateral elements for the plastically deformable billet. Material behavior was defined by previously calibrated flow-stress curves from the prior work [11]. To capture radial diameter change and springback induced by actuation, the segmented sleeve and die were modeled as elastic bodies, while the remaining tool components were idealized as rigid. A mesh-convergence study indicated that an element size of 0.3 mm was sufficient, as further refinement did not affect the predicted ejection forces. Comparable element sizes were used for the sleeve and die to ensure stable contact. The press kinematics were prescribed via a time–stroke table, and the infeed of the active reinforcement was applied by an axial force F_{ax}. Figure 2 summarizes the infeed curve for the axial infeed force obtained from preliminary numerical and experimental trials. The friction coefficient μ in Figure 2 refers to the interface between the elastically modeled segmented sleeve and the active reinforcement; because the 2D idealization represents the sleeve as a continuous solid, an effective steel–steel friction coefficient of μ = 0.02 was used to match the experimentally measured infeed curve. Based on the numerical and experimental results in Figure 2 (left), an axial cushion displacement of 2.5 mm requires approximately 100 kN, and in unloaded conditions the resulting radial actuation reduces the die inner diameter by about 40 µm, thereby lowering clamping pressure and ejection forces [7].

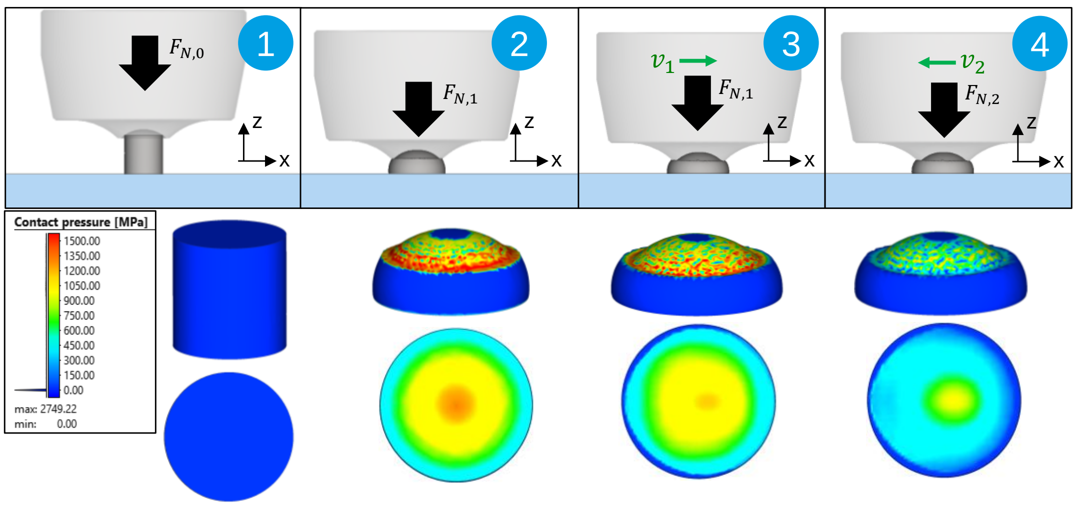

Figure 3 Sliding compression test setup and two stage model test procedure. Left: Tribometer including the relevant units. Right: Process sequence consisting of upsetting, forward sliding and reverse sliding at normal load.

Tribological characterization was performed using a sliding compression test depicted in Figure 3. A cylindrical specimen, typically 15 mm × 15 mm, is upset against a sliding plate under a prescribed normal force and subsequently displaced laterally over a defined stroke. The friction coefficient μ is obtained from the measured normal and tangential forces. The setup enables systematic variation of the tribological load via normal force, lubricant system, sliding kinematics, and, if required, temperature by heating the plate [1, 5]. To represent the ejection stage and the reduced clamping pressures enabled by the adaptive die in Figure 1, the test sequence was modified to include a forward sliding segment followed by a one-second dwell. Next, the normal force was adjusted to the target condition, and a subsequent reverse sliding segment was added. The sliding distance was set to 50 mm in both directions, and all tests were conducted at room temperature without tool heating.

Since the characteristic contact pressure cannot be obtained directly from the tribometer instrumentation, a three-dimensional FE model of the upset sliding test was used to determine the reference pressure levels. The model setup and the flow stress curve for 16MnCr5 were adopted from the preceding publication [9]. In the FE model, the specimen was treated as a deformable body, whereas the sliding plate and punch were idealized as rigid. Simulations were carried out with the implicit solver in Simufact Forming 2024.4 using a hexahedral mesh. Based on a mesh-convergence study, a discretization of approximately 8,500 elements was selected because further refinement mainly increased computation time without changing the mean contact pressure used for evaluation. The normal load was applied via a phase-dependent, adjustable spring force in the z-direction acting through the sliding plate, while the sliding motion was prescribed by the punch. The initial friction coefficient was set to the experimentally identified value determined in this study for the respective condition. Transferability between real trials and model tests was ensured by matching characteristic contact pressures.

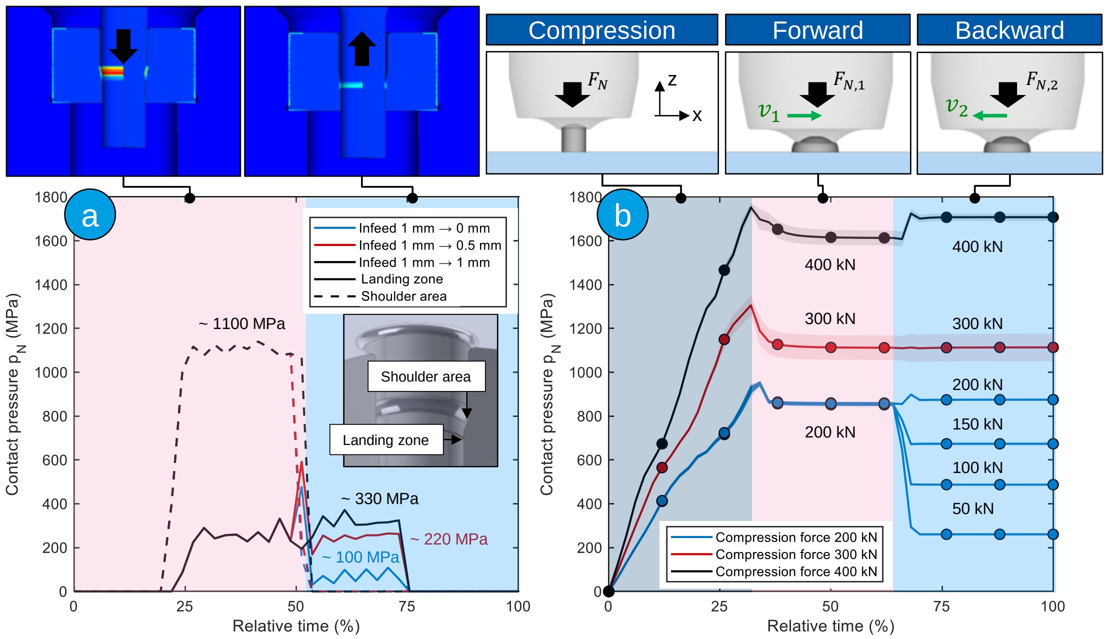

Figure 4 Characteristic normal contact pressures used for transfer from the numerical results: (a) Contact pressures during tapering for the main forming stage and the ejection stage. (b) Contact pressures obtained for the compression stage at different load levels and for the individual phases of the two-stage sliding compression test.

In the tapering process, pressures were evaluated phase specifically using the two-dimensional FE model above [6]. During the main forming stroke (0 – 50 % relative time), the average shoulder pressure was used as the representative value, whereas for the ejection stage (> 50 %) the landing-zone clamping pressure was evaluated, see Figure 4a. By reducing radial actuation during ejection, the landing-zone pressure drops from approximately 330 MPa to 50 MPa, see Figure 4a. A comparable trend is observed in the model test during the return stroke: for the blue case, decreasing the upsetting force from 200 kN to 50 kN reduces the contact pressure from about 825 MPa to 210 MPa, see Figure 4b. Based on these results, characteristic pressures were assigned separately to the forward and reverse segments as a function of compression force and fitted by a second-order polynomial. This calibration enables the selection of an upsetting force that reproduces a target pressure level from the real process, thereby ensuring a load-consistent transfer of friction results to both forming and ejection conditions.

3 Results and Discussion

Figure 5 summarizes the reference tribometer results obtained with the sliding compression test for the single-layer lubricant system PD5940. Figure 5a reports the friction coefficients for the forward stroke, Figure 5b for the backward stroke, and Figure 5c the ratio μ_b/μ_f to facilitate comparison between both directions. All tests shown in Figure 5 were conducted at a normal contact pressure of 801 MPa for the material 16MnCr5 in forward direction. For consistent comparison across Figure 5a–c, the x-axis lists only the contact pressure assigned to the backward stroke. Consequently, the forward stroke data in Figure 5a represents identical tribological loading conditions from left to right. Only successful tests were included in the averaging procedure used to determine the characteristic friction coefficient μ. In the forward stroke, a mean friction coefficient of μ = 0.057 with an uncertainty of Δμ = 0.01 was obtained for material 16MnCr5, see Figure 5a in blue. The relatively large scatter is consistent with prior reports for single-layer systems, since the absence of a zinc-phosphate carrier layer means that the polymer film alone must separate tool and billet and is therefore sensitive to local variations in coating thickness, contact temperature, contamination, and surface conditioning [5].

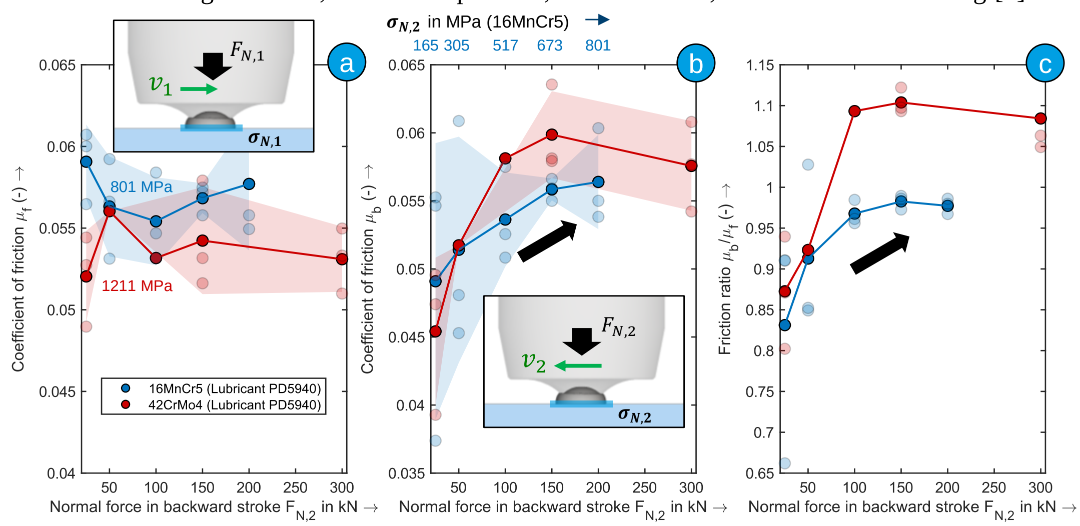

Figure 5 Results of the two-stage sliding compression test for the polymer-based lubricant, with N = 3 repetitions for 16MnCr5 and 42CrMo4: (a) Friction coefficient in the forward stroke. (b) Friction coefficient in the backward stroke. (c) Friction ratio

In contrast, the backward stroke in Figure 5b exhibits an increasing friction coefficient with increasing contact pressure. Raising the pressure from 165 MPa to 801 MPa for 16MnCr5 increases the friction coefficient by Δμ = 0.005 - 0.015, while at low pressures the backward stroke friction remains clearly below the forward stroke mean value. This trend is highlighted by the ratio μ_b/μ_f in Figure 5c, which reduces the influence of forward stroke scatter while preserving the coupling between both directions. The observed pressure dependence contradicts common literature trends that typically report decreasing friction with increasing pressure and cannot be explained directly by the usual viscosity reduction argument for polymer lubricants, indicating the need for a more detailed analysis of the reverse stroke contact conditions [1, 5]. To assess material effects, the same test series was repeated with 42CrMo4, which exhibits higher flow stress than 16MnCr5. The corresponding results, shown in red in Figure 5, confirm the same pressure-induced increase in reverse stroke friction, demonstrating that the phenomenon is not governed by the billet material. Figure 6 examines whether the pressure-dependent friction trend observed in the backward stroke in Figure 5 can be attributed to residual lubricant on the sliding plate or to a surface modification generated during the preceding load cycle. In the sliding compression test, the preloaded specimen and the lubricant state from the forward stroke slide again over the same plate surface in the reverse stroke. Therefore, the presence of remaining lubricant films, local roughening, or incipient wear could, in principle, affect friction. This has already been discussed for cold forging tribometers where lubricant residues on the tool surface can measurably change the coefficient of friction [1]. To isolate these effects, two consecutive forward strokes were performed on identical plates (Phase I and Phase II), while varying the configuration between phases. The plate orientation was either kept constant (forward-forward), rotated by 180 degrees (forward-backward), or the plate was cleaned and polished to a defined reference surface before Phase II (forward-new plate). Because the setup change required several minutes, both specimen and plate cooled to room temperature before Phase II. Under these conditions, Phase II shows the literature consistent trend of decreasing friction with increasing contact pressure, and no systematic influence of plate orientation or cleaning was detected, see Figure 6c. Consequently, neither remaining lubricant nor the surface state produced by Phase I represents the dominant cause of the friction increase with pressure observed in the reverse stroke of Figure 5.

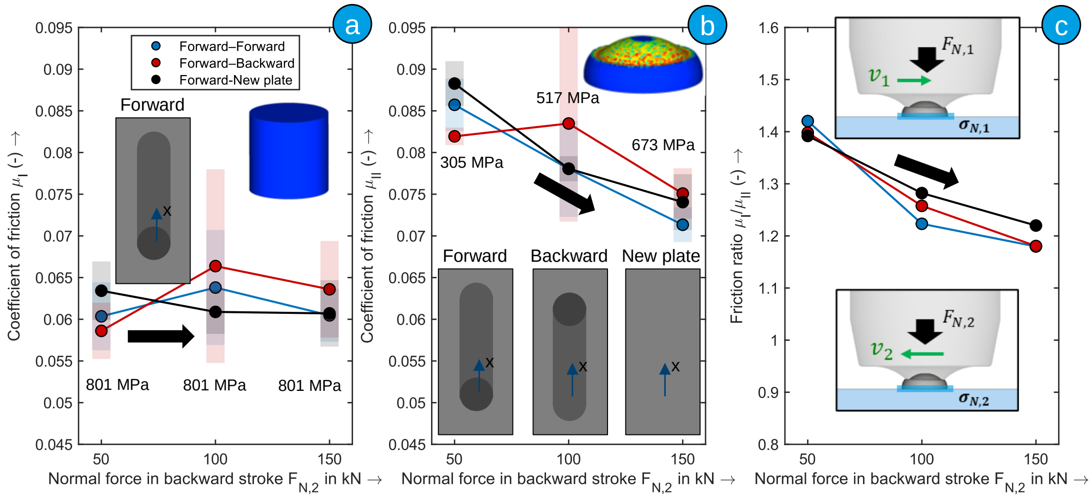

Figure 6 Sensitivity study of the two-stage model test under different Phase II conditions, with N = 3 repetitions for 16MnCr5 (PD5940): (a) Friction coefficients in Phase I (forward stroke). (b) Friction coefficients in Phase II for the modified plate configurations. (c) Friction ratio between Phase II and Phase I.

The key difference between Figures 5 and 6 is the thermal history of the contact and the continuity of the interface. In Figure 5, the backward stroke follows the forward stroke after only 1 s without separating the specimen from the sliding plate. Thus, the contact enters the reverse motion with pronounced thermal preloading and an unchanged interfacial state. In contrast, the specimen in Figure 6 was removed between Phases I and II, and the specimen and plate were cooled to near room temperature before the second stroke. In the process of cold forging, frictional work and plastic deformation can locally raise interface temperatures well above ambient. As a result, polymer-based lubricant films may exhibit two competing effects: moderate heating can lower shear resistance and reduce friction, whereas exceeding a lubricant-specific temperature limit can trigger thermal or chemical degradation, impair film integrity, and increase friction again [12]. Such temperature-driven performance loss has been reported for dry-film and dry-in-place lubricant systems, with marked changes already around 100 °C due to depletion of friction modifiers and antiwear additives [5]. Consistent with this mechanism, higher contact pressures in the reverse stroke are expected to promote higher flash temperatures, accelerating degradation and explaining both the friction increase with pressure in Figure 5 and the occurrence of lubricant failure with friction values exceeding μ = 0.1. In addition to thermal effects, the inverse pressure-dependent friction response may be influenced by pressure-induced reconfiguration of the lubricant film prior to the reverse stroke. Following axial forming observations in [13], reducing contact pressure during unloading can homogenize the lubricant layer in the deformation zone and restore a more uniform separation film. This interpretation is consistent with reduced process forces reported for axial forming compared with conventional forward extrusion and supports the inverse contact-pressure friction trend observed in Figure 5.

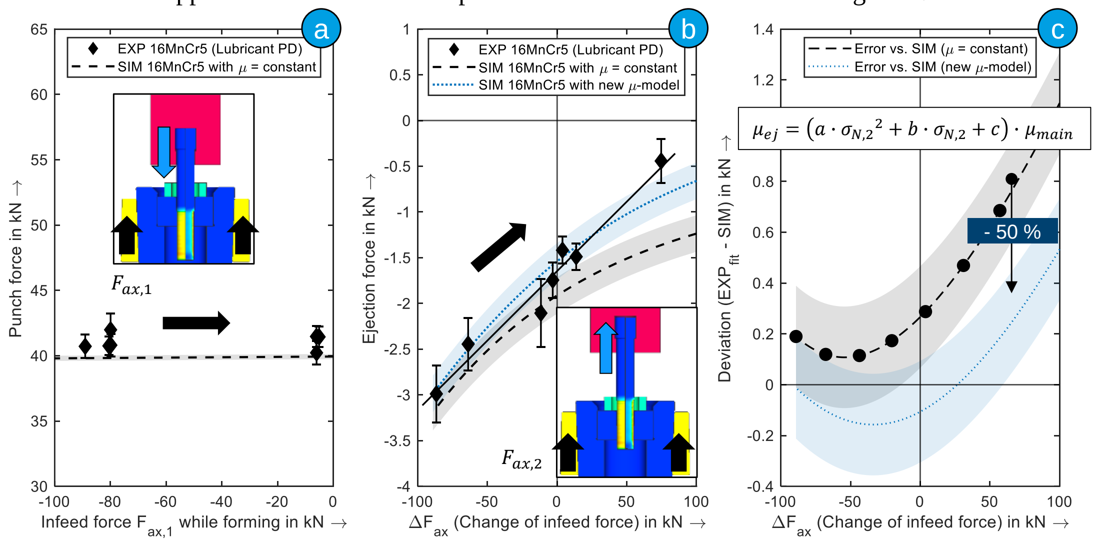

Figure 7 Process force response of the adaptive extrusion die and validation of the friction correction for the ejection stage: (a) Punch forces during the forward stroke. (b) Ejection forces as a function of the preload change. (c) Deviation between experimental and FE predicted forces, including the proposed μ-correction model.

To transfer the model test findings to the real forming process, Figure 7 compares force data from the main forming stage and the ejection stage for different prestress settings of the adaptive extrusion die, quantified by the infeed force of the flexible reinforcement. Figure 8a shows both numerical and experimental results indicating that the main forming force is essentially insensitive to the preload adjustment. A change of the die inner diameter by only a few micrometers does not alter the die's macroscopic geometry. Therefore, it has no measurable effect on the press force, which is consistent with the geometric considerations in Figure 6. Figure 7b presents the ejection force as a function of the change in infeed force, $\Delta F_{ax} = F_{ax,1} - F_{ax,2}$. The case ΔF_{ax} = 0 kN corresponds to the reference condition without preload modification, whereas positive values represent a reduction of die preload, since the external pressure, and thus elastic die springback, decrease. Experimentally, increasing ΔF_{ax} from 0 to 100 kN leads to an approximately linear reduction of the ejection force. In contrast, FE-predictions obtained with a constant friction coefficient of μ = 0.06 exhibit a pronounced quadratic trend, causing the deviation between simulation and experiment to increase with ΔF_{ax}, as quantified in Figure 7c. Based on the friction trends identified in Figure 5 and the pressure mapping established in Figure 4, Figure 7c shows the introduction of a dedicated friction correction for the ejection stage.

The approach assigns a pressure-dependent corrected friction coefficient derived from the upset sliding test and applies this value as a constant during the ejection stage in the tapering simulations. In this way, a new constant ejection-phase friction coefficient $\mu_{ej,}$ is defined based on the friction $\mu_{main,}$ identified for the main forming stage and the associated contact pressure, while explicitly accounting for the pressure change from the main stroke to the onset of ejection. To select the appropriate corrected friction coefficient for each prestress setting, the characteristic contact pressure in the landing zone is extracted from the corresponding FE simulations as a function of ΔF_{ax}. As shown by the deviation evaluation in Figure 7c, the proposed correction reduces the ejection force prediction error by approximately a factor of two.

4 Conclusion and Outlook

The model tests provide new insights into the tribological mechanisms governing the ejection stage and enable the following conclusions:

- The adaptive extrusion die reduces ejection forces not only by lowering clamping pressure via reduced prestress, but also by decreasing the friction coefficient when polymer-based lubricants are used.
- The mechanism is attributed to thermal preloading of the interface during the main stroke, which can degrade polymer lubricants at high subsequent pressures and increase friction. Conversely, unloading and reduced contact pressure prior to the reverse stroke may enable partial lubricant film recovery, resulting in a more uniform separation layer and lower friction.
- The results further indicate that residual lubricant on the tool surface, the alignment of the preloaded tool surfaces, and topography modifications generated during the main stroke have a secondary influence on the identified friction trend. The dominant factor is the resulting contact pressure level.
- The impact of the main stroke on the ejection stage can be captured by a friction coefficient correction approach. This enables a more accurate representation of the ejection phase in finite element simulations and supports improved prediction of ejection forces.

Acknowledgments

This work was supported by the Deutsche Forschungsgemeinschaft (DFG, German Research Foundation) in the framework of the priority program SPP 2013 („Residual stresses“) by a grant OE 558/16-2, GR 1818/63-2 and GR 1818/86-1 (531874276).

References

[1] A. J. P. G. Christoph Müller, "Lubrication of Cold Forging Tools with Single Layer Lubricants," *46th ICFG Plenary Meeting,* p. 31, 2013.

[2] M. L. N. M. H. V. Tahsin Deliktas, "Investigation on the Influence of the Tribological System on Cold Forging and Ejection of Hollow Components with Helical Internal Geometry," *Defect and Diffusion Forum,* no. Vol. 414, pp. 155-162, 2022.

[3] S. O. B. C. Chengliang HU, "Evaluation of dry-in-place lubricants for cold forging by using an optimal steady combined forward and backward extrusion testing method," *Friction,* no. 10, p. 1862–1876, 2023.

[4] L. Dubar, A. Dubois and M. Dubar, "Tribology of Forward Extrusion – from the Identification of Friction to the Prediction of Abrasive and Adhesive Wear," *Proceedings of the 9th JSTP International Seminar on Precision Forging (ISPF 2024) March 11–14 2024, Kyoto, Japan,* 2024.

[5] P. Groche, S. Zang, C. Müller and D. Bodenmüller, "A study on the performance of environmentally benign lubricants at elevated temperatures in bulk metal forming," *Journal of Manufacturing Processes,* p. 425–430, 2015.

[6] W. Volk, Targeted Use of Forming-induced Residual Stresses in Metal Components, Munich: Technical University of Munich, 2024.

[7] P. K. W. S. P. G. Christoph Kuhn, "Ejection tribology (Tribologie des Ausstoßens)," *massivUMFORMUNG*, pp. 56 - 60, Dezember 2022.

[8] A. Franceschi, J. Stahl, C. Kock, R. Selbmann, S. Ortmann-Ishkina, A. Jobst, M. Merklein, B. Kuhfuß, M. Bergmann, B.-A. Behrens, W. Volk and P. Groche, "Strategies for residual stress adjustment in bulk metal forming," *Arch Appl Mech (Archive of Applied Mechanics)*, no. 8, p. 3557–3577, 2021.

[9] D. Molitor, S. Volz, J. Launhardt and P. Groche, "Maschinelles Lernen in der Tribologie/Machine learning in tribology," *wt (wt Werkstattstechnik online)*, p. 643–648, 2022.

[10] Ö. N. Cora, M. Akkök and H. Darendeliler, "Modelling of variable friction in cold forging," *Proceedings of the Institution of Mechanical Engineers, Part J: Journal of Engineering Tribology*, p. 899–908, 2008.

[11] V. S. G. P. M. P. L. J. B. N. Hu Chengliang, "Modeling of friction in cold forging considering a wide range of tribological conditions," in *ICFG - International Cold Forging Group 55th Plenary Meeting*, Milan - Italy 2022, 2022.

[12] P. Martins Ferreira, Q. Arnoux, C. Charrin, B. Trindade and M. Kalin, "Lubrication of polyphthalamide (PPA) and polyetheretherketone (PEEK) with biodegradable synthetic esters: Effects of base oil polarity, temperature and polymer aging," *Tribology International*, no. 200, pp. 1 - 13, 2024.

[13] B. H. Peter Groche, "Friction control for accurate cold forged parts," *CIRP Annals - Manufacturing Technology*, no. 63, pp. 285-288, 2014.